Ordered Micro/Nanostructured Arrays Based on the Monolayer Colloidal Crystals†

Yue Li,* Weiping Cai,* and Guotao Duan

Key Laboratory of Materials Physics, Institute of Solid State Physics, Anhui Key Laboratory of Nanomaterials and Nanotechnology, Chinese Academy of Sciences, Hefei, 230031, Anhui, China

Received July 24, 2007. Revised Manuscript Received September 6, 2007

Besides the traditional lithographical techniques to fabricate the ordered mciro/nanostructured arrays, the route of the monolayer colloidal crystal template is a recently promising, alternative process for the synthesis of the micro/nanostructures with different designed morphologies. By this strategy, two-dimensional ordered arrays, e.g., nanoparticle arrays, pore arrays, nanoring arrays, nanobowl arrays, hollow sphere arrays, etc., even one-dimensional nanostructures of ordered nanorod/nanopillar/nanowire arrays, etc., could be prepared. Recent progress in this area is reviewed, including synthesis strategies and morphology-dependent properties of the micro/nanostructured arrays such as optical properties, wettability, surface-enhanced Raman scattering, and photonic bandgap.

Introduction

Two dimensional (2D) ordered micro/nanostructured arrays have recently received considerable attention because of their many applications in biosensors, magnetic materials, phonon diffraction grating, photonic crystals, drug delivery, surface-enhanced Raman scattering (SERS), etc.[1] Their properties are morphology- and arrangement-parameter-dependent and hence the morphology-controlled fabrication with a large area becomes more important. In the conventional techniques, the most widely used method is photolithography; unfortunately, it can not be widely applied to the nanostructured synthesis because of its diffraction-limited resolution, ca. $\lambda/2$ (λ is photowavelength).[2] Besides this, electron beam lithography, X-ray lithography, scanning tunneling microscopy, and atomic force microscopy lithography are alternative methods.[3] Although they have abilities to create the nanostructured arrays with high quality, they can not be afforded by most laboratories because of their high costs and low sample throughout. Additionally, soft lithography[4] including the techniques of replica molding (REM),[5] microcontact printing (μCP),[6] micromolding in capillaries (MIMIC),[7] etc., has been developed to fabricate the micro/nanostructured arrays. This route has advantages of cheapness, high resolution, and high repetition; however, a micro/nanopatterned elastomer used as the mask, stamp, or mold must be preprepared in this process,[4–7] which restricts its applications to some extent.

Recently, many researchers have developed some other parallel strategies mainly based on self-assembly processes.[8] One of these routes, a monolayer colloidal crystal (MCC) template approach, has attracted more interests to fabricate the ordered arrays with well-defined micro/nanostructures because of its flexibility and controllable morphologies.[9]

As we know, with the development of the colloidal science, the highly monodispersed colloidal spheres with a size deviation less than 5% of diverse materials such as silica, polystyrene (PS), and PMMA have been easily synthesized in liquid media by various methods.[10] The successful synthesis of the monodispersed colloidal spheres makes it easy to fabricate the colloidal crystals by a self-assembly with various methods such as drop-coating,[11] spin-coating,[12] dip-coating,[13] and electrophoretic deposition[14,15] and therefore further improves their applications. The typical MCC is an ordered monolayer colloidal microsphere array with a hexagonal close-packed (hcp) alignment on a certain substrate. Moreover, the fabrication techniques of a non-close-packed (ncp) MCC are also explored.[16] Jiang et al. developed the method to prepare ncp MCC by a combination of spin-coating and monomer photopolymerization.[16a] Yang et al. utilized the solvent-swelling and mechanical deformation behaviors of PDMS to adjust the lattice structures of the 2D arrays of microspheres and prepared the ncp MCCs with the hexagonal or square arrangements.[16b] Ong et al. prepared the ncp MCCs composed of nonspherical particles by reactive ion etching of the MCCs.[16d] These MCCs could be directly used as the optical grating, optical filter, and antireflective coating. More importantly, they can be used as flexible templates to prepare the various ordered structured arrays. Since Deckman et al. prepared an ordered microcolumn arrays by the PS MCC as a mask using so-called natural lithography in 1982,[17] the MCC template strategy has been developed to synthesize a plentiful 2D ordered structures including nanoparticle arrays, pore arrays, nanobowl arrays, nanoring arrays, hollow sphere arrays, nanopillar arrays, hierarchical micro/nanoparticle arrays, etc., by different methods such as evaporation/sputtering deposition, electrochemical deposition, and solution/sol dipping deposition. Interestingly, for its further extension, using nanoparticle arrays obtained by MCC as mask or catalysts, one-dimensional (1D) nanostructured arrays, e.g., ordered nano-

† Part of the "Templated Materials Special Issue".

* Corresponding auther. E-mail: yueli@issp.ac.cn (Y.L.); wpcai@issp.ac.cn (W.C.).

10.1021/cm701977g CCC: $40.75
Published on Web 11/08/2007

Scheme 1. Fabrication of Ordered Nanoparticle Arrays Based on the Evaporation/Sputtering Deposition on the MCC: (a) MCC, (b) Element Deposition, (C) Nanoparticle Arrays after Removing the MCC Mask

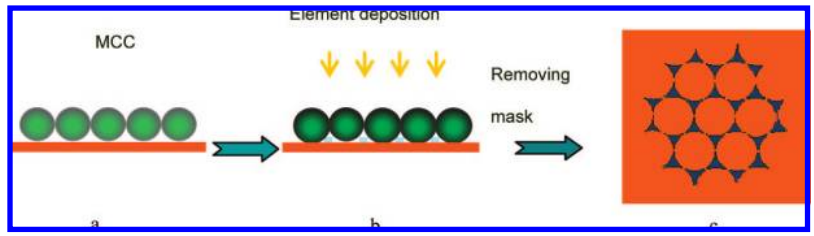

pillar/nanorod/nanowire arrays and carbon nanotube arrays, etc., could be grown on the solid substrates by reactive ion etching or chemical vapor deposition. In the strategy of the MCC templates, the periodicities of arrays can be tuned by changing the diameter of the colloid sphere in the templates and the morphologies could be well-controlled by the experimental conditions. Until now, the MCC template technique has proved to be a successful and promising one to fabricate the ordered micro/nanostructured arrays.

In previous studies, the ncp MCC templates mainly focused on the fabrication of the ordered pore array films[16] and the MCC templates with hcp arrangements were more widely developed to fabricate the ordered micro/nanostructured arrays with various morphologies. In this brief review, the recent developments of the template technique of the MCC with a hcp alignment are presented, mainly including (1) 2D ordered micro/nanostructured arrays such as nanoparticle arrays, pore arrays, nanowall arrays, and hollow sphere arrays, by the various methods; (2) 1D nanostructured ordered arrays by the MCC; (3) morphology-dependent properties of the micro/nanostructured arrays.

1. 2D Ordered Micro/Nanostructured Arrays

1.1. Strategy of the Direct MCC Templates or Masks. The hcp MCCs were directly used as masks or templates to fabricate the 2D ordered nanostructured arrays by the different methods, e.g., evaporation deposition, solution/sol dipping deposition, electrodeposition, etc. After the templates or masks were removed, the 2D ordered arrays with diverse morphologies could be created.

Evaporation/Sputtering Deposition or Reactive Ion Etching. The ordered nanoparticle arrays can be formed on substrates after the evaporation/sputtering deposition of elements on the MCCs and subsequent removal of the masks,[18] as shown in Scheme 1. Figure 1 presents a gold nanoparticle array with the hexagonal arrangement with a *P6mm* symmetry and triangular cross-section. In addition, using this method, we could fabricate bimetal nanoparticle arrays by changing the evaporating source in the second-half process of deposition.[18a]

In this approach, the nanoparticle distribution density can be increased using smaller periodicity of the MCC masks, and the volume of a single nanoparticle in the array could be tuned by controlling the metal evaporation quantity.

Inversely, by reactive ion etching, an ordered triangular nanopore or nanowell array can be created on the substrate using the MCC as a mask,[19] as displayed in Figure 2.

Solution/Sol Dipping Deposition.[20] If a droplet of the precursor solution/sol is dropped onto a MCC, the MCC template will float on the solution/sol surface because of the surface tension of the solution/sol. After the template is dried and then removed (for organic colloidal spheres, the template could be removed by calcinations and/or dissolution), the ordered structures can thus be obtained. The fabrication process is illustrated in Scheme 2. The morphologies of the ordered structured arrays can be controlled by the solution/sol concentration and the sphere deformation during the drying process.[20a] By this method, the ordered micro/nanostructured arrays (films) with different materials such as metal, semiconductor, even polymer, etc., can be produced. With a decrease in the precursor concentration from a high level to a very low one, pore arrays, through pore arrays, and ring arrays could, in turn, be obtained. Figure 3 shows the typical ordered pore array and nanoring array by the solution/sol dipping deposition.[20a,b] By this method, the ordered pore arrays of Fe_2O_3, TiO_2, silica, Al_2O_3, In_2O_3, ZnO, Co_2O_3, CuO, CeO_2, Eu_2O_3, and Dy_2O_3, and even polymers such as PDMS, could be fabricated.

Additionally, besides the flat substrates, the ordered pore array films can be synthesized on the curved surfaces to further develop this technique.[21] The fabrication process was displayed in Scheme 3. A MCC on a glass substrate was peeled off in the precursor solutions and floated on the

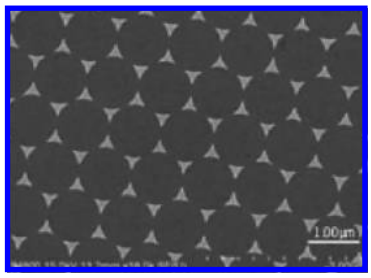

Figure 1. Gold nanoparticle array fabricated by the PS MCC with the PS size of 1μm. Reprinted with permission from ref 18a. Copyright 2005 Springer.

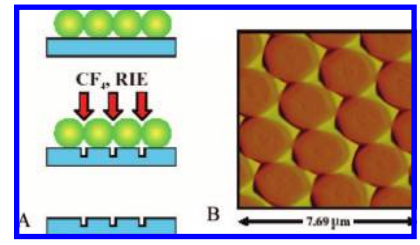

Figure 2. Nanowell array by reactive ion etching (RIE). (A) RIE scheme. (B) AFM image of the nanowell array. Reprinted with permission from ref 19. Copyright 2001 Materials Research Society.

Scheme 2. Schematic Illustrations of the Solution/Sol Deposition: (i) MCC on a Substrate, (ii) MCC Floating on the Surface of the Precursor Solution/Sol, (iii) Integrity of the Solute/Gel and the MCC, (iv) Ordered Micro/Nanostructured Array Film

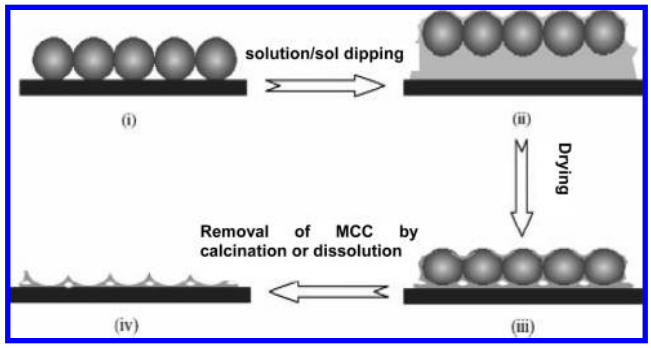

precursor solution. The interstitial space between the close-packed spheres was filled by the solution because of the capillary effects. The floating MCC was then picked up by any desired substrate with a flat or curved surface (here, a ceramic tube is used) and the MCC covered the tube surface by filling the precursor solution in the interstitial space among the colloidal spheres and the space between the MCC template and curved surface. Subsequently, the sample was dried at a temperature slightly above the glass transition of PS spheres and finally calcined to remove the colloidal template.

For instance, using a 0.1 M $SnCl_4$ precursor solution and the MCC with a diameter of 1000 nm, the ordered pore films of SnO_2 were fabricated on the curved surface, as shown in Figure 4 on the outer (Figure 4A) and inner (Figure 4B) surfaces of a glass tube, for example, on a spherical surface (Figure 4C), as well as a flat surface (Figure 4D), respectively. Apparently, the microstructures of all the ordered porous films on the curved surfaces are similar. The pore openings at the film surfaces are nearly circular. For these films, after being heated at 500 °C for 1 h, they adhere so strongly to the curved surfaces that they cannot be removed or destroyed, even by ultrasonic washing.

Electrodeposition.[22] Scheme 4 illustrates a typical electrodeposition route based on the MCC template. A MCC is first self-assembled on a cleaned glass substrate, transferred from the glass substrate to a conductive one, such as ITO glass, and then heated for a given time at a certain temperature, leading to it being fixed firmly on the new substrate. Finally, this conductive substrate is used as the working electrode in a three-electrode electrolytic cell, with a graphite plate or metal foil as the auxiliary electrode, a saturated calomel electrode (SCE) as the reference electrode, and the aqueous electrodeposition solution as the electrolyte. After electrodeposition at a constant electric potential or a constant electric current for a certain time and then removal of the MCC template, the 2D ordered arrays can be generated on the conductive substrates.

We fabricated gold through-pore arrays by the electrodeposition after removing the PS MCC using a solution composed of $AuCl_4$ (12 g L^{-1}), EDTA (5 g L^{-1}), Na_2SO_3 (160 g L^{-1}), and K_2HPO_4 (30 g L^{-1}) as the electrolyte, as shown in Figure 5A. With an increase in the heating time of the MCC template, the opening pores evolve from an irregular shape to circles and the pore size also increases because of a heating-induced rise in contact area between the PSs and the substrate. The film thickness and openings at the film surface can be controlled by the electrodeposition time. Additionally, a zinc oxide nanowall array was synthesized using the corresponding electrolyte by this route (Figure 5B). If one chooses a solution composed of 0.01 M $NiCl_2$ and 0.03 M $(NH_4)_2SO_4$ as the electrolyte and keeps the pH value to 8.5 with ammonia, then the Ni hollow sphere array could be produced (Figure 5C) at a low cathodic current density (J). Additionally, a 1 M $Ni(NO_3)_2$ aqueous solution acts as the electrolyte and its pH value is adjusted to 1.7 with nitric acid. The cathodic current density is controlled to 1.2 mA/cm^2. After the electrodeposition and removal of the MCC, an ordered $Ni(OH)_2$ hollow sphere array with hierarchical micro/nanostructure could be created (Figure 5D).

In addition to the above materials, other metal and metal oxide pore array films (Ag, Eu_2O_3, CdS, Fe_2O_3, etc.) could be synthesized by the electrodeposition based on the MCC template using the corresponding electrolyte.[22]

In addition, other approaches have been developed for the synthesis of the ordered micro/nanostructured arrays based on the MCC.[23] For example, using the MCC as a microlens array, researchers could fabricate the ordered arrays such as pore arrays and nanobump arrays on the substrates by laser irradiation;[23a–e] polymer ordered structured arrays can be created by in situ polymerization using the MCC template;[23f,g] sphere arrays with the nanohole on each sphere top could be produced by selective etching;[23h–j] binary nanoparticle arrays and decoration of nanoparticles on sphere arrays were prepared by the combination of etching and deposition.[23k,l]

1.2. Two-Step Replication Strategy Based on the MCC Templates.[24] In this approach, a MCC is used as the first template to fabricate 2D ordered micro/nanostructures, such as pore arrays and nanobowl arrays, and then these ordered structures are applied for the synthesis of other orderly structured arrays as the second templates or masks. By this method, nanoparticle arrays, nanoring array, and hollow sphere arrays could be fabricated on the substrates.

Wang et al. fabricated the liftable TiO_2 nanobowl array sheet by the atomic layer deposition, subsequent ion milling, and finally etching using the MCC as the first template. Each nanobowl has a hole at its bottom in the array (see the inset in Figure 6A) and the whole nanobowl array sheet can be lifted from its supporting substrate by introducing a thin organic layer between the nanobowls and the substrate. The hole size at the bottom of the nanobowl can be controlled by the experimental conditions. Using this sheet as a mask, researchers were able to create ordered nanodot patterns with the designed sizes by element deposition (Figure 6A).[24a] Goedel et al. applied the silica MCC as the first template to fabricate the polymer closely packed ordered pore array membranes (inset in Figure 6B), and they used the porous membranes as the second template for the synthesis of

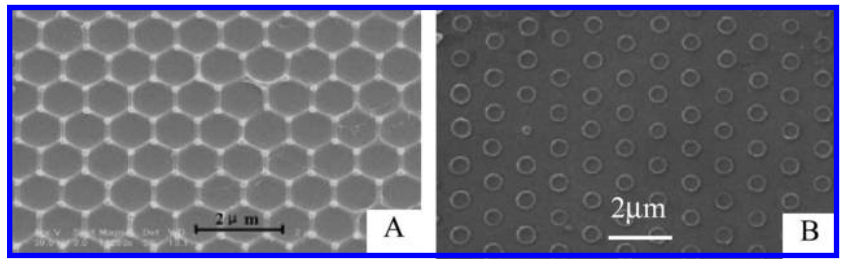

Figure 3. (A) Fe_2O_3 ordered pore array by the precursor ($Fe(NO_3)_3$ solution concentration of 0.06 M. Reprinted with permission from ref 20a. Copyright 2004 Wiley-VCH. (B) TiO_2 nanoring array by the TiO_2 sol concentration of 0.05 M. Reprinted with permission from ref 20b. Copyright 2006 American Chemical Society.

Scheme 3. Route to Fabricate a Porous Structured Array on the Curved Surface: (i) Flat Glass Substrate Covered with a PS Sphere MCC was Dipped into the Solution; (ii) MCC Floated onto the Precursor Solution Surface; (iii) Monolayer Is Picked up Using a Ceramic Tube; (iv) Tube with the Monolayer and Solution Was Heated in a Furnace; (v) Ordered Pore Array Film Was Formed on the Tube Surface after Heat Treatment and Removal of the MCC Template (Reprinted with permission from ref 21. Copyright 2005, Wiley-VCH)

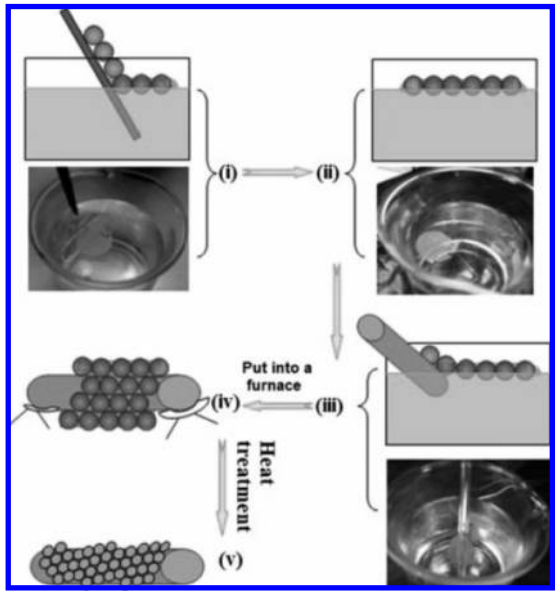

mesoscopic gold rings (Figure 6B) by filling the pores with a solution of gold precursor (0.25 wt % $HAuCl_4$ in ethanol) and calcinations at 450 °C.[24b]

Recently, we created an Al_2O_3 pore array on ITO glass using the MCC template by the solution-dipping method, and then used it as the secondary template to synthesize the Ni hollow sphere array (Figure 6C) and pore array (Figure 6D) using electrodeposition.[24c] By the same method, Au a hierarchical micro/nanoparticle array was also fabricated by the electrodeposition using various electrolyte after removal of the second template (Figure 6E).[24d] The FeO(OH) pore arrays, which were obtained by the MCC solution dipping route, were also used as the second template, filling the polymer solution in the pores and then drying them. The polymer hollow sphere arrays could be fabricated after the removal of the secondary membranes, as shown in Figure 6F.[24e] Interestingly, with a decrease in the polymer precursor solution, a hole will gradually appear on the top of each hollow sphere and the corresponding hole size will increase, which could be useful in microreactor devices that can endure acidic and alkaline conditions, selective permeability, and nutrient and drug delivery.

2. Ordered One-Dimensional (1D) Nanostructured Arrays

1D ordered nanostructured arrays could also be produced that were based on the MCC template technique. Using the 2D nanostructured arrays (e.g., nanoparticle arrays) obtained by the MCC template method as previously described as the mask or catalysts, one can synthesize 1D ordered structured arrays (e.g., nanotube arrays,[25] nanowire arrays,[26] nanorod or nanopillar arrays,[27] hollow pillar arrays,[28] etc.) by reactive ion etching or chemical vapor deposition. These 1D nanostructured arrays have a great variety of applications, especially in photonic crystals, field emitters, and piezoelectric nanogenerators.

For example, Ren et al. first prepared the Ni nanoparticle arrays using the MCCs as masks and then synthesized the large-area periodic arrays of well-aligned carbon nanotubes by the hot filament PECVD method using the Ni nanoparticle arrays as catalysts, as shown in Figure 7A.[25] Chen et al. fabricated the large-area well-ordered periodic nanopillar arrays based on the combination of the MCC template method and etching technique.[27a] They created Al nanoparticle arrays by the MCC masks and then, taking these Al nanoparticle arrays as the second masks, prepared the silicon nanopillar arrays on a silicon wafer by the reactive ion etching process using a mixture of CHF_3 and O_2 (Figure 7B). Goedel et al. fabricated the polymer pore arrays on the silicon wafer using the MCCs as masks and then deposited gold on the pore arrays on the supporting substrate. After the removal of the polymer pore arrays, the gold nanodot patterns remained on the substrate and the silicon pillar arrays with a large area were obtained by a deep reactive ion etching process using them as the masks, as shown in Figure 7C.[27c]

Moreover, utilizing the orderliness of the monolayer colloidal crystal, nanopillar arrays can be fabricated on the top of the MCC by the glancing angle deposition (GLAD).[29] Gall et al. deposited the Si onto a MCC from an angle α of 72° with respect to the surface normal; the substrate was rotated about the polar axis at a speed of 60 rpm, and the Si nanopillar arrays were fabricated on the MCCs, as displayed in Figure 7D.[29a]

Besides the above methods, the nanopillar arrays have been synthesized making use of the triangle channels of the heat-deformed MCCs.[30] In this method, at first, the MCCs are synthesized on the substrates and then heated at a temperature

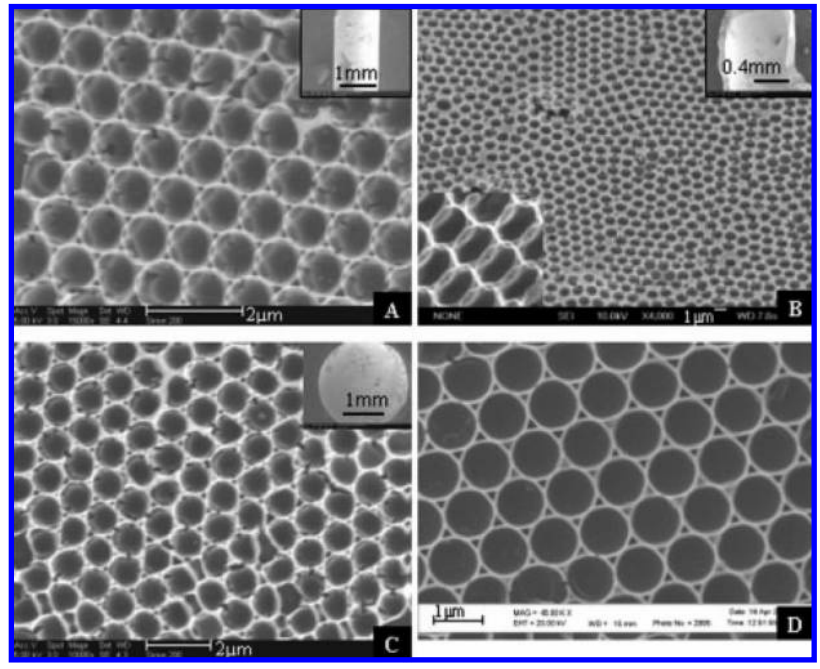

Figure 4. FESEM images of SnO_2 ordered pore array films on the curved surfaces: (A) on the outer surface of a glass tube (diameter 1.2 mm); (B) on the inner surface of a glass tube (diameter 1.0 mm); (C) on the surface of a steel sphere (diameter 2.5 mm); and (D) on a flat surface. The insets show the corresponding low-magnification images. Diameters of the PS spheres are 1000 nm. Reprinted with permission from ref 21. Copyright 2005 Wiley-VCH.

Scheme 4. Schematic Illustration of the Electrodeposition Based on the MCC: (A) MCC on the Substrate; (B) MCC Transferred on a Conductive Substrate; (C) MCC Fixed on the Conductive Substrate by Heating; (D) Design of the Cathode; (E) Electrodeposition in a Cell; (F) Ordered Array after the Removal of the MCC Template (Reprinted with permission from ref 22a. Copyright 2004 Wiley-VCH.)

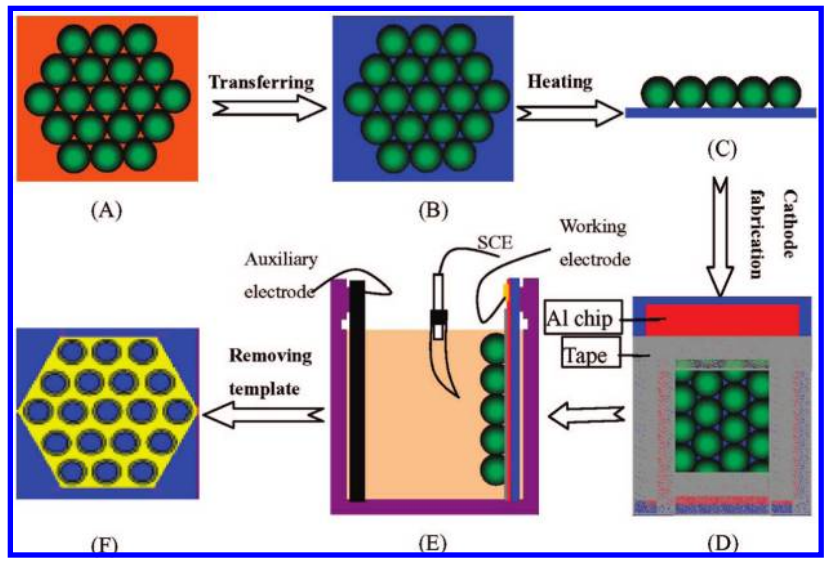

(e.g., 120 °C for PS) above the glass transition, T_g (T_g of PS = 100 °C) for a certain time, after which the MCCs will be deformed so much that the triangular prism channels can be formed at the interstices among them. Using these MCCs with the channels as the templates, periodic nanopillar arrays can then be directly fabricated by the solution/sol-dipping deposition.

3. Properties of Ordered Micro/Nanostructured Arrays

Some properties, such as the surface wettability, optical properties, surface-enhanced Raman scattering, and photonic bandgaps, have also been investigated on the basis of these ordered structured arrays. These properties are closely morphology- and arrangement-parameter-dependent. Their investigations supply useful theoretic foundations for their further applications on micro/nanodevices based on the ordered structured arrays.

3.1. Wettability. The wettability of solid surfaces is an important property depending on both chemical compositions and the surface structure. Generally, the wettability is associated with the surface roughness for a certain material. Especially, superhydrophobic surfaces (contact angle (CA) larger than 150°) have attracted much attention for the

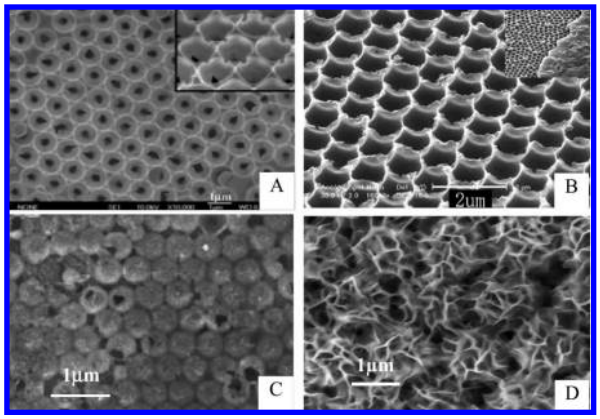

Figure 5. Ordered nanostructured arrays by the electrodeposition based on the MCCs. (A) Au through-pore array. Reprinted with permission from ref 22a. Copyright 2004 Wiley-VCH. (B) ZnO nanowall array. Reprinted with permission from ref 22b. Copyright 2004 Royal Society of Chemistry. (C) Ni hollow sphere array. Reprinted with permission from ref 22d. Copyright 2006 American Chemical Society. (D) hierarchical $Ni(OH)_2$ hollow sphere array. Reprinted with permission from ref 22d. Copyright 2007 Wiley-VCH.

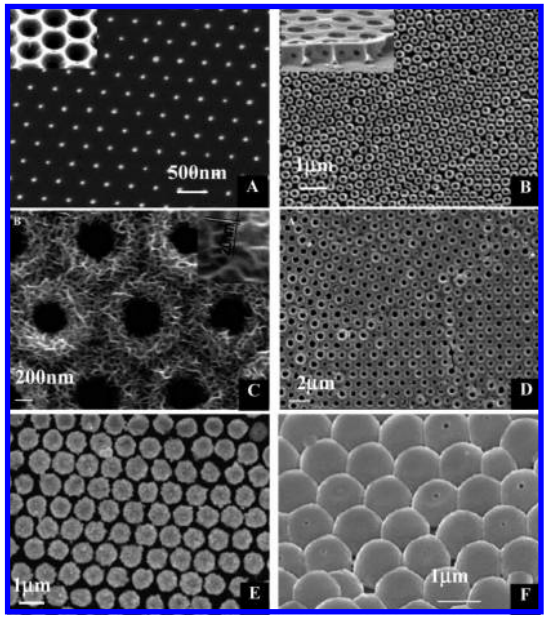

Figure 6. Ordered micro/nanostructured arrays by the two-step replication based on the MCC. (A) Au nanodot array; inset, the second template of the TiO_2 nanobowl array. Reprinted with permission from ref 24a. Copyright 2005 American Chemical Society. (B) Au nanoring array; inset, polymer porous membrane. Reprinted with permission from ref 24b. Copyright 2004 American Chemical Society. (C) Ni hollow sphere array. Copyright 2006 American Chemical Society. (D) Ni pore array. Reprinted with permission from ref 24c. Copyright 2006 American Chemical Society. (E) Au hierarchical micro/nanoparticle array. Reprinted with permission from ref 24d. Copyright 2006 American Institute of Physics. (F) PVA hollow microsphere array. Reprinted with permission from ref 24e. Copyright 2005 Materials Research Society.

fundamental interest and practical applications, such as the prevention of the adhesion of snow and raindrops to antennas and windows and the creation of self-cleaning, antioxidation, and microfluidic devices. For the fabrication of the superhydrophobic surfaces, it is necessary to create the rough structures on a hydrophobic surface (CA > 90°) and lower the surface energy by chemical modification, such as coating with fluoroalkylsilanes or thiol. As we know, a great number of orderly structured array films based on the MCC (e.g.,

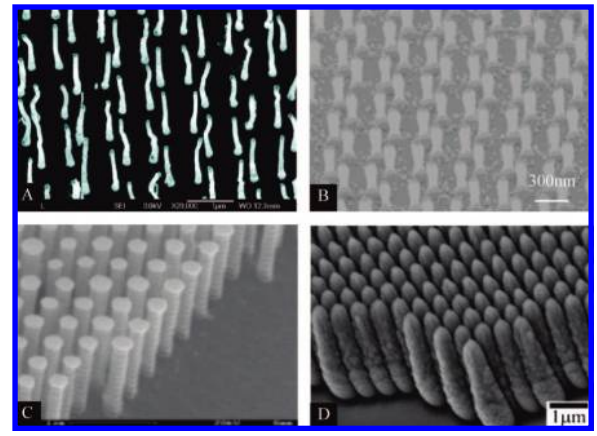

Figure 7. (A) Ordered carbon nanotube array grown by PECVD. Reprinted with permission from ref 22. Copyright 2003 American Institute of Physics. (B) silicon nanopillar array by reactive ion etching. Reprinted with permission from ref 27a. Copyright 2003 American Chemical Society. (C) Si nanopillar array by reactive ion etching using gold dot pattern as mask. Reprinted with permission from ref 27c. Copyright 2007 American Institute of Physics. (D) Si nanopillar on the MCC by GLAD. Reprinted with permission from ref 29. Copyright 2006 Elsevier.

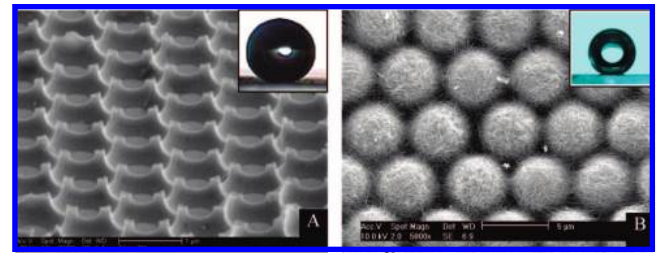

Figure 8. (A) Silica pore film with nanopillar array. Reprinted with permission from ref 31. Copyright 2006 Institute of Physics. (B) Bionic hierarchical microsphere/SWCNT composite array film. Reprinted with permission from ref 35a. Copyright 2007 American Chemical Society. The insets are corresponding water droplet shape after chemical modification with the low-free-energy materials.

pore array films,[31] ordered pillar array films,[30] periodic nanoparticle arrays,[32] etc.) are rough on the micro/nanoscales and could induce superhydrophobicity. Recently, we found that the wettability of the silica pore array films can be controlled by the roughness caused by the heating deformation of the MCC.[31a] The roughness of the pore arrays increased with the increase in deformation of the PS MCC template in a certain range, and the corresponding superhydrophobicity would be enhanced after modification with low surface free energy materials, as displayed in Figure 8A. For ZnO pore array films, the roughness of the porous film increased with an increase in the precursor concentration, and strong superhydrophobicity with a water contact angle of 165° was obtained when the precursor concentration was 1.0 M. Meanwhile, a photoinduced reversal transition of the wettability between hydrophobicity and hydrophilicity was also observed on the zinc oxide pore array films.[31b] Moreover, Mulvaney et al. investigated the wettability of nanoparticle arrays by the MCC template technique. They found that the nanoparticle array film led to large increases in the water CA and generated superhydrophobicity with a CA larger than 150° after modification.[32]

The surface of a MCC cannot induce superhydrophobicity because of its low roughness factor. However, the nanopar-

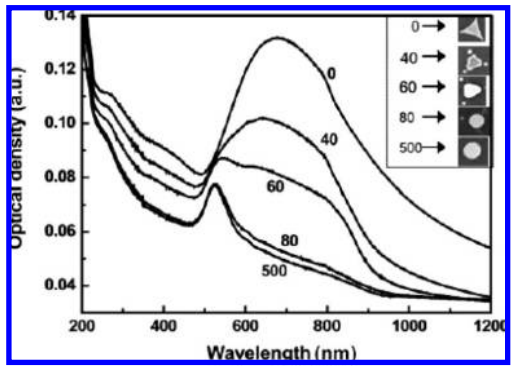

Figure 9. Evolution of the optical spectra of the gold particle arrays on quartz versus the laser irradiation with the indicated number of laser pulses. Inset: the corresponding morphology of individual dots at each pulse number. Reprinted with permission from ref 18a, copyright 2005 Springer.

ticles or nanotubes are decorated on spherical surfaces of the MCC by different methods (e.g., photochemical method,[33] sputtering deposition,[34] wet chemical self-assembly,[35] and heating decomposition[36] etc.), the hierarchical micro/nanostructured arrays would be prepared, which is similar to the surface structure of a lotus leaf, and the corresponding roughness was increased largely compared to the MCC. After modification, these surfaces could display a strong superhydrophobicity with a lotus effect. For instance, Cho et al. fabricated single-walled carbon nanotubes on the PS sphere surfaces of MCC by a wet chemical self-assembly technique and subsequently chemically modified the surface with a low-surface-energy material; the morphology of the synthesized bionic surface bore much resemblance to natural lotus leaves and hence the wettability exhibited a remarkable superhydrophobicity, as displayed in Figure 8B.

3.2. Surface Plasmon Resonance Absorption. Noble metal nanoparticles have pronounced surface plasmon resonance (SPR) absorption, which has potential applications in many fields, such as optical waveguides and optical switches. In general, SPR absorption is highly dependent on the nanoparticle size, shape, interparticle spacing, and dielectric constants of the materials. Using the MCC as a mask, the noble metal nanoparticle array such as silver, gold bimetal of silver, and gold could be easily fabricated by the evaporation deposition. In this method, the particle size and interparticle spacing can be tuned by changing the periodicity of the MCC, and the nanoparticle shape could be controlled by thermal annealing or laser irradiation.

Van Duyne et al. synthesized the silver nanoparticle arrays and systematically investigated the effects of silver particle size, shape, interparticle spacing, nanoparticle–substrate interaction, solvent, dielectric overlayers, and molecular adsorbates on localized surface plasmon resonance absorption.[9a,18d–18f,37] Our group prepared gold nanoparticle arrays and the morphologies of the particle arrays could be manipulated by laser irradiation.[18a] With an increase in the number of laser pulses, the particle shape changed from a triangle to a polyhedron and finally to a nearly spherical shape. The corresponding optical absorption spectra are shown in Figure 9, with the particle shape changing by the laser irradiation. The gold nanoparticle arrays show a very broad absorbance peak centered around 680 nm together with a shoulder extending well into the near-infrared region, which

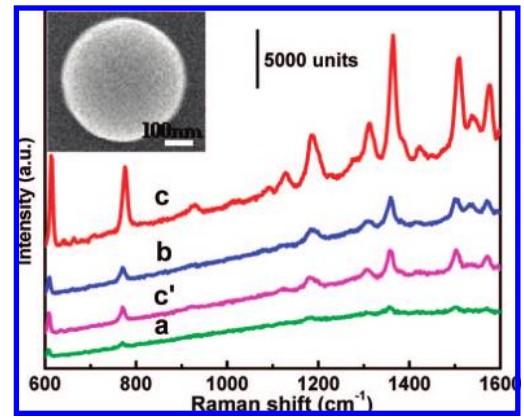

Figure 10. SERS spectra of R6G on diverse substrates. (a) smooth Au film; (b) rough Au film; (c and c′): Au particle array before and after laser irradiation. Inset: the FESEM image of a single Au particle in the array after 532 nm laser irradiation (15 mJ/cm^2 per pulse) for 800 shots. Reprinted with permission from ref 24d. Copyright 2006 American Institute of Physics.

indicates that the peak is composed of at least two peaks. The peak at 680 nm decreases and disappears as the laser irradiation is increased up to 100 pulses. In addition, after irradiation by about 60 pulses, another peak emerges around 550 nm. After about 100 pulses, the peak shifts to 530 nm. Generally, spherical particles have only a single SPR peak at ca. 530 nm. In these results, the broad absorption band around 680 nm for the sample before irradiation can be attributed to the superposition of the two bands of the triangular-shaped particles. The laser irradiation makes the particles spheroidize, leading to a decrease and eventual disappearance of the shape dependent band around 680 nm, leaving only the single SPR band at 530 nm corresponding to a spherical particle. The variations in spectra can reflect the morphological changes of the particle arrays and, further, the related information of the laser, which shows the potential application of such a method in the fabrication of data storage devices.

3.3. Surface-Enhanced Raman Scattering. The surface-enhanced Raman scattering (SERS) is a powerful technique for sensitive and selective detection of low concentration analytes and hence has many applications in the identification of organic pigments and dyes, single molecule detection and the fields of sensors, biotechnology, and nanodevices. Generally, the SERS is related to the SERS-active substrate, a kind of rough surface, such as the particle film. Recently, ordered arrays have proved to be good candidates for the SERS-active substrates due to the periodic characteristic and the nanosized structure. For example, the metal nanoparticle arrays and metallic ordered coating arrays have been synthesized and have shown the importance in the application of the SERS.[38] The success of these applications strongly relies on the material and the size of the array, and also on the fine structure of the building blocks in the array. Additionally, the hierarchically structured ordered particle array, with the microsized building blocks and the nanosized fine structure or the surface roughness, should present important applications in the SERS.

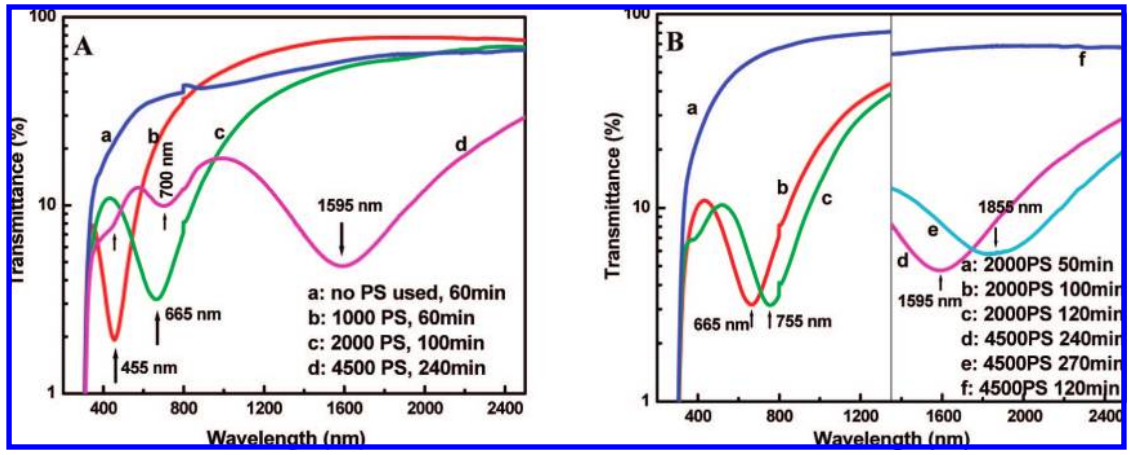

Figure 11. Optical transmission spectra of $Ni(OH)_2$ samples on an ITO glass with the incident light perpendicular to the substrate. Reprinted with permission from ref 22e. Copyright 2007 Wiley-VCH.

For instance, the hierarchically micro/nanostructured rough Au particle array fabricated by the electrodeposition using an alumina pore array as the second template (shown in Figure 6E) exhibits a strong SERS effect using Rhodamine 6G (R6G) as probe molecules, as demonstrated in Figure 10.[24d] For comparison, the results for a smooth Au film, prepared by the vacuum physical vapor deposition on the ITO substrate, and a rough Au film, prepared by the electrodeposition on the ITO substrate without the MCC template using the same deposition parameters, were also measured. The smooth Au film gives only a very weak signal (curve a). With respect to the rough Au film, the signal remains relatively weak but stronger than that of the smooth Au film because of its nanoscaled surface roughness (curve b). The hierarchical micro/nanoroughness gold film, however, exhibits a very strong SERS signal (curve c), which is much stronger than that of the rough Au film. The morphology of the Au particle shows spherical shape with the smooth surface after proper laser irradiation, as shown in the inset of Figure 10. The corresponding SERS intensity was decreased dramatically (curve c′ in Figure 10), suggesting that the nanosized surface roughness of the microparticles is also a favorable factor for the SERS. Further experiments have demonstrated that when the R6G concentration is down to 1×10^{-8} M, the hierarchical rough Au particle array still shows the obvious Raman signals, whereas no any signal can be detected for the rough Au film or the sample of the hierarchical rough particle array after the laser irradiation. The strong SERS for the hierarchical rough particle array can be attributed to both the periodic structure and the hierarchical surface roughness.

3.4. Tunable Optical Transmission Stop Band. The hierarchically micro/nanostructured $Ni(OH)_2$ monolayer hollow sphere arrays could be synthesized by the electrodeposition, as shown in Figure 5D.[22e] The monolayer hollow sphere arrays can demonstrate tunable optical properties in a large region, as displayed in Figure 11. A size-dependent optical transmission stop band exists in the hierarchically structured hollow sphere arrays, which red-shifts in a large range from 455 to 1595 nm with the size increase of the hollow spheres in the array from 1000 to 4500 nm. Interestingly, the position of the stop band can also be fine-

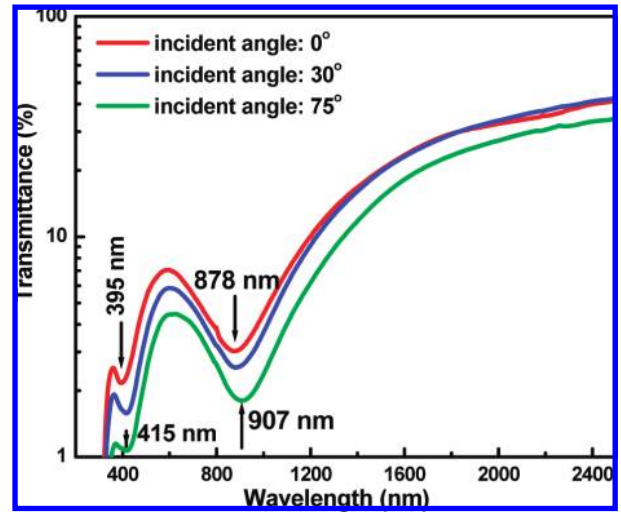

Figure 12. Optical transmission spectra of $Ni(OH)_2$ sample on the ITO glass with different incident angles (the angle between the incident light and the normal to the sample plane, θ). It has two clear transmission stop bands due to first and second diffractions, which is beneficial to the understanding of the shift of stop band. Reprinted with permission from ref 22e. Copyright 2007 Wiley-VCH.

adjusted by the deposition time without the change of the periodicity. The increase in the deposition time leads to a red-shift of the band for the hollow sphere arrays, as shown in curves b–e of Figure 11B, which could be due to the denser shell of the hollow sphere. This indicates that the optical transmission stop band could be flexibly controlled in a large region, by the PS's size for coarse-tuning and the deposition time for fine adjustment. Importantly, further experiments show that the position of the transmission stop band is almost independent of the incident angle θ, as shown in Figure 12. This incident-angle-independent position of the stop band, which 3D photonic crystals do not possess, should be of great significance for applications in optical devices, photonic crystals, nanoscience, and nanotechnology.

As we know, an optical transmission stop band will be found in a 3D colloidal crystal (or an inverse opal structure) but cannot be produced in a 2D monolayer colloidal crystal. The hierarchical monolayer hollow sphere array can equivalently be considered as symmetrical double layers (a top layer and a bottom layer) with the interspacing d, as shown in

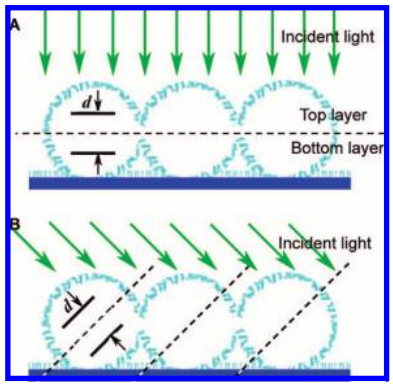

Figure 13. Schematic illustration of the double-layer photonic crystal approximation for the hollow sphere array. (A) Incidence of light perpendicular to the sample plane ($\theta = 0$); (B) A slant incidence of light ($\theta > 0$). Reprinted with permission from ref 22e. Copyright 2007 Wiley-VCH.

Figure 13, indicating a photonic crystal with the double layers. Under perpendicular incidence of a light beam (or $\theta = 0$, see Figure 13A), the diffraction equation can written as $m\lambda_{min} = 2nd$, where n corresponds to the mean refractive index of the layers (consisting of sphere shell and interstice). Although the exact values of n (the mean refraction index) and d (the periodical constant along the normal of the sample plane) are unknown, the d value should increase with a rise in the PS size, and n depends on material species and the structure of the shell. Obviously, the denser the sphere shell (or the longer the deposition time), the larger the n value. Thus, for the first-order diffraction ($m = 1$), the transmission stop band should red-shift with an increase in the sphere size or the deposition time.

As for the θ-independent stop band, it was attributed to the special structure of the monolayer hollow sphere. Because of the symmetry of the hollow spheres, for the incident light with different θ, the d value should be similar (see Figure 13B) and thus the position of the stop band is almost independent of θ.

Conclusions and Outlook

The MCC template technique has proved to be an inexpensive, flexible, and portable strategy to fabricate the ordered micro/nanostructured arrays. On the basis of the MCC templates, a series of plentiful ordered structured arrays with different morphologies (e.g., nanoparticle arrays, pore arrays, hollow sphere arrays, nanoring arrays, hierarchical sphere arrays, nanopillar arrays, nanotube arrays, nanowire arrays, etc.) can be synthesized, combined with other techniques such as the evaporation/sputtering deposition, solution/sol deposition, electrodeposition, and active ion etching. The morphologies of these micro/nanostructured arrays can be well-controlled by changing the experimental conditions, i.e., the diameter of the colloidal sphere in the MCC, the concentration of precursor solution/sol, the heating time of the MCC, the recipe of the electrolyte, the electrodeposition time, etc. Moreover, some important properties, which are morphology- or microstructure-dependent, such as optical properties, wettability, and surface-enhanced Raman scattering, have been investigated. These structures could be useful in applications for energy storage or conversion, data storage, next-generation integrated nanophotonics devices, biomolecular labeling and identification, microfluidic devices, catalysts, microreactor devices, miniaturized optical components, self-cleaning surface, etc.

Although the fabrication techniques for the micro/nanostructured arrays based on the MCCs have been well-developed, there still exists a big space to prepare new micro/nanostructured arrays by combining colloidal templates with other techniques such as etching, laser/electron beam irradiation, pulsed laser deposition, etc. Compared to the amount of research on the synthesis, there has not been much investigation of the properties and nanodevices dependent on ordered structured arrays. As the evolution of the MCC template technique is still ongoing, novel ordered arrays and excellent properties will also be expected. Especially, it is hoped that the micro/nanodevices can be developed based on these ordered structured arrays.

Acknowledgment. This work was supported by the Major State research program of China "Fundamental Investigation on Micro-Nano Sensors and Systems based on BNI Fusion" (Grant No. 2006CB300402) and the Knowledge Innovation Program of the Chinese Academy of Sciences (Grant No. KJCX2-SW-W31), Anhui Provincial Natural Science Foundation of China (Grant No. 070414199), the National Natural Science Foundation of China (Grant No. 50601026, No. 50671100).

References

(1) (a) Haes, A. J.; Van Duyne, R. P. *Mater. Res. Soc. Symp. Proc.* **2002**, *723*, O3.1.1. (b) Mailly, D.; Chaperlier, C.; Benoit, A. *Phys. Rev. Lett.* **1993**, *70*, 2020. (c) Vu, P. D.; Olson, J. R.; Pohl, R. O. *Ann. Phys.* **1995**, *4*, 9. (d) Yablonovitch, E.; Gmitter, T. J.; Meade, R. D.; Rappe, A. M. *Phys. Rev. Lett.* **1991**, *67*, 80. (e) Tessier, P. M.; Velev, O. D.; Kalambur, A. T. *Adv. Mater.* **2001**, *13*, 396. (f) Duan, G. T.; Cai, W. P.; Li, Y.; Cao, B. Q. *J. Nanosci. Nanotechnol.* **2006**, *6*, 2474. (g) Tanaka, M.; Motomura, T.; Kawada, M.; Anzai, T.; Shiroya, T.; Shimura, K.; Onishi, M. *Biomaterials* **2000**, *21*, 1471. (h) Wang, D.; Caruso, F. *Adv. Mater.* **2001**, *13*, 350. (i) Cho, S. O.; Jun, H. Y.; Ahn, S. K. *Adv. Mater.* **2005**, *17*, 120.

(2) Wallraff, G. M.; Hinsberg, W. D. *Chem. Rev.* **1999**, *99*, 1801.

(3) (a) Smith, H. I.; Schattenburg, M. L. *IBM J. Res. Dev.* **1993**, *37*, 319. (b) Stroscio, J. A.; Eigler, D. M. *Science* **1991**, *254*, 1319. (c) Liu, G.-Y.; Xu, S.; Qian, Y. *Acc. Chem. Res.* **2000**, *33*, 457. (d) Piner, R. D.; Zhu, J.; Xu, F.; Hong, S.; Mirkin, C. A. *Science* **1999**, *283*, 661.

(4) (a) Xia, Y. N.; Whitesides, G. M. *Angew. Chem., Int. Ed.* **1998**, *37*, 550. (b) Weibel, D. B.; DiLuzio, W. R.; Whitesides, G. M. *Nat. Rev. Microbiol.* **2007**, *5*, 209.

(5) Xia, Y. N.; Whitesides, G. M. *Langmuir* **1997**, *13*, 2059.

(6) (a) Kumar, A.; Whitesides, G. M. *Appl. Phys. Lett.* **1993**, *63*, 2002. (b) Quist, A. P.; Pavlovic, E.; Oscarsson, S. *Anal. Bioanal. Chem.* **2005**, *381*, 591.

(7) Kim, E.; Xia, Y.; Whitesides, G. M. *Nature* **1995**, *376*, 581.

(8) Wang, Z. L. *Adv. Mater.* **1998**, *10*, 13.

(9) (a) Haynes, C. L.; Van Duyne, R. P. *J. Phys. Chem. B* **2001**, *105*, 5599. (b) Winzer, M.; Kleiber, M.; Dix, N.; Wiesendanger, R. *Appl. Phys. A: Mater. Sci. Process.* **1996**, *63*, 617. (c) Burmeister, F.; Badowsky, W.; Braun, T.; Wieprich, S.; Boneberg, J.; Leiderer, P. *Appl. Surf. Sci.* **1999**, *144–145*, 461. (d) Burmeister, F.; Schafle, C.; Keilhofer, B.; Bechinger, C.; Boneberg, J.; Leiderer, P. *Adv. Mater.* **1998**, *10*, 495. (e) Boneberg, J.; Burmeister, F.; Schafle, C.; Leiderer, P. *Langmuir* **1997**, *13*, 7080. (f) Xu, H.; Goedel, W. A. *Small* **2005**, *1*, 808. (g) Wang, Y.; Han, S.; Briseno, A. L.; Sanedrin, R. J. G.; Zhou, F. *J. Mater. Chem.* **2004**, *14*, 3488. (h) Yan, Q. F.; Chen, A.; Chua, S. J.; Zhao, X. S. J. *Nanosci. Nanotechnol.* **2006**, *6*, 1815. (i) Yang, S. M.; Jang, S. G.; Choi, D. G.; Kim, S.; Yu, H. K. *Small* **2006**, *2*, 458. (j) Zhang, X.; Whitney, A. V.; Zhao, J.; Hicks, E. M.; Van Duyne, P. R. *J. Nanosci. Nanotechnol.* **2006**, *6*, 1. (k) Wang, X. D.; Graugnard, E.; King, J. S.; Wang, Z. L.; Summers, C. J. *Nano Lett.* **2004**, *4*, 2223.

(10) (a) Stöber, W.; Fink, A. *J. Colloid Interface Sci.* **1968**, *26*, 62. (b) Zou, D.; Derlich, V.; Gandhi, K.; Park, M.; Sun, L.; Kriz, D.; Lee, Y. D.; Kim, G.; Aklonis, J. J.; Salovey, R. *J. Polym. Sci. Part A: Polym. Chem.* **1990**, *28*, 1909. (c) Arshady, R. *Colloid Polym. Sci.* **1992**, *270*, 717.

(11) (a) Micheletto, R.; Fukuda, H.; Ohtsu, M. *Langmuir* **1995**, *11*, 3333. (b) Rakers, S.; Chi, L. F.; Fuchs, H. *Langmuir* **1997**, *13*, 7121. (c) Denkov,

N. D.; Velev, O. D.; Kralchevsky, P. A.; Ivanov, I. B.; Yoshimura, H.; Nagayama, K. *Langmuir* **1992**, *8*, 3183. (d) Denkov, N. D.; Velev, O. D.; Kralchevsky, P. A.; Ivanov, I. B.; Yoshimura, H.; Nagayama, K. *Nature* **1993**, *361*, 1303. (e) Hulteen, J. C.; Van Duyne, R. P. *J. Vac. Sci. Technol.* **1995**, *13*, 1553. (f) Haynes, C. L.; Van Duyne, R. P. *J. Phys. Chem. B* **2001**, *105*, 5599.

(12) (a) Ozin, G. A.; Yang, S. M. *Adv. Funct. Mater.* **2001**, *11*, 95. (b) Jiang, P.; McFarland, M. J. *J. Am. Chem. Soc.* **2004**, *126*, 13778. (c) Wang, D.; Möhwald, H. *Adv. Mater.* **2004**, *16*, 244. (d) Mihi, A.; Ocana, M.; Mí guez, H. *Adv. Mater.* **2006**, *18*, 2244. (e) Jiang, P. *Chem. Comm.* **2006**, 1699. (f) Hulteen, J. C.; Van Duyne, R. P. *J. Vac. Sci. Technol., A* **1995**, *13*, 1553. (g) Li, Y.; Cai, W. P.; Duan, G. T.; Sun, F. Q.; Cao, B. Q.; Lu, F. *Mater. Lett.* **2005**, *59*, 276.

(13) (a) Antony, S.; Dimitrov, A. S.; Nagayama, K. *Langmuir* **1996**, *12*, 1303. (b) Jiang, P.; Bertone, J. F.; Hwang, K. S.; Colvin, V. L. *Chem. Mater.* **1999**, *11*, 2132. (c) Kralchevsky, P. A.; Denkov, N. D. *Curr. Opin. Colloid Interface Sci.* **2001**, *6*, 383. (d) Im, S. H.; Kim, M. H.; Park, O. O. *Chem. Mater.* **2003**, *15*, 1797. (e) Kitaev, V.; Ozin, G. A. *Adv. Mater.* **2003**, *15*, 75. (f) Denkov, N. D.; Velev, O. D.; Kralchevsky, P. A.; Ivanov, I. B.; Yoshimura, H.; Nagayama, K. *Langmuir* **1992**, *8*, 3183. (g) Ko, H.; Lee, H. W.; Moon, J. *Thin Solid Films* **2004**, *447–448*, 638.

(14) Choi, W. M.; Park, O. O. *Nanotechnology* **2006**, *17*, 325.

(15) (a) Binks, B. P.; Horozov, T. S. *Colloidal Particles at Liquid Interfaces*; Cambridge University Press: Cambridge, U.K., 2006. (b) Chabanov, A. A.; Jun, Y.; Norris, D. J. *Appl. Phys. Lett.* **2004**, *84*, 3573. (c) Meng, L.; Wei, H.; Nagel, A.; Wiley, B. J.; Scriven, L. E.; Norris, D. J. *Nano Lett.* **2006**, *6*, 2249. (d) Prevo, B. G.; Hon, E. W.; Velev, O. D. *J. Mater. Chem.* **2007**, *17*, 791. (e) Ormonde, A. D.; Hicks, E. C. M.; Castillo, J.; Van Duyne, R. P. *Langmuir* **2004**, *20*, 6927. (f) Kondo, M.; Shinozaki, K.; Bergström, L.; Mizutani, N. *Langmuir* **1995**, *11*, 394.

(16) (a) Jiang, P.; McFarland, M. J. *J. Am. Chem. Soc.* **2005**, *127*, 3710. (b) Yan, X.; Yao, J.; Lu, G.; Li, X.; Zhang, J.; Han, K.; Yang, B. *J. Am. Chem. Soc.* **2005**, *127*, 7688. (c) Ren, Z.; Li, X.; Zhang, J.; Zhang, X.; Yang, B. *Langmuir* **2007**, *23*, 8272. (d) Tan, B. J.-Y.; Sow, C.-H.; Lim, K.-Y.; Cheong, F.-C.; Chong, G. L.; Wee, A. T.-S.; Ong, C.-K. *J. Phys. Chem. B* **2004**, *108*, 18575.

(17) Deckman, H. W.; Dunsmuir, J. H. *Appl. Phys. Lett.* **1982**, *41*, 377.

(18) (a) Sun, F.; Cai, W.; Li, Y.; Duan, G.; Nichols, W. T.; Liang, C.; Koshizaki, N.; Fang, Q.; Boyd, I. W. *Appl. Phys. B: Lasers Opt.* **2005**, *81*, 765. (b) Burmeister, F.; Schäfle, C.; Matthes, T.; Böhmisch, M.; Boneberg, J.; Leiderer, P. *Langmuir* **1997**, *13*, 2983. (c) Pacifica, J.; Gómez, D.; Mulvaney, P. *Adv. Mater.* **2005**, *17*, 415. (d) Jensen, T. J.; Duval, M. L.; Kelly, K. L.; Lazarides, A. A.; Schatz, G. C.; Van Duyne, R. P. *J. Phys. Chem. B* **1999**, *103*, 9846. (e) Malinsky, M. D.; Kelly, K. L.; Schatz, G. C.; Van Duyne, R. P. *J. Phys. Chem. B* **2001**, *105*, 2343. (f) Hulteen, J. C.; Treichel, D. A.; Smith, M. T.; Duval, M. L.; Jensen, T. J.; Van Duyne, R. P. *J. Phys. Chem. B* **1999**, *103*, 3854. (g) Tan, B. J. Y.; Sow, C. H.; Koh, T. S.; Chin, K. C.; Wee, A. T. S.; Ong, C. K. *J. Phys. Chem. B* **2005**, *109*, 11100. (h) Sort, J.; Glaczynska, H.; Ebels, U.; Dieny, B.; Miersig, M.; Rybczynski, J. *J. Appl. Phys.* **2004**, *95*, 7516.

(19) (a) Haes, A. J.; Haynes, C. L.; Van Duyne, R. P. *Mater. Res. Soc. Symp.* **2001**, *636*, D4.8.1. (b) Whitney, A. V.; Myers, B. D.; Van Duyne, R. P. *Nano Lett.* **2004**, *4*, 1507.

(20) (a) Sun, F. Q.; Cai, W. P.; Li, Y.; Cao, B. Q.; Lei, Y.; Zhang, L. D. *Adv. Funct. Mater.* **2004**, *14*, 283. (b) Sun, F. Q.; Yu, J. C.; Wang, X. C. *Chem. Mater.* **2006**, *18*, 3774. (c) Li, Y.; Cai, W. P.; Duan, G. T.; Sun, F. Q.; Lu, F. *Appl. Phys. A: Mater. Sci. Process.* **2005**, *81*, 269. (d) Li, Y.; Cai, W. P.; Cao, B. Q.; Duan, G. T.; Li, C. C.; Sun, F. Q.; Zeng, H. B. *J. Mater. Chem.* **2006**, *16*, 609. (e) Sun, F. Q.; Cai, W. P.; Li, Y.; Cao, B. Q.; Lei, Y.; Zhang, L. D. *Mater. Sci. Technol.* **2005**, *21*, 500.

(21) Sun, F. Q.; Cai, W. P.; Li, Y.; Jia, L. C.; Lu, F. *Adv. Mater.* **2005**, *17*, 2872.

(22) (a) Sun, F. Q.; Cai, W. P.; Li, Y.; Cao, B. Q.; Lu, F.; Duan, G. T.; Zhang, L. D. *Adv. Mater.* **2004**, *16*, 1116. (b) Cao, B. Q.; Cai, W. P.; Sun, F. Q.; Li, Y.; Lei, Y.; Zhang, L. D. *Chem. Commun.* **2004**, 1604. (c) Cao, B. Q.; Sun, F. Q.; Cai, W. P. *Electrochem. Solid-State Lett.* **2005**, *8*, G237. (d) Duan, G. T.; Cai, W. P.; Li, Y.; Li, Z. G.; Cao, B. Q.; Luo, Y. Y. *J. Phys. Chem. B* **2006**, *110*, 7184. (e) Duan, G. T.; Cai, W. P.; Luo, Y. Y.; Sun, F. Q. *Adv. Funct. Mater.* **2007**, *17*, 644.

(23) (a) Piglmayer, K.; Denk, R.; Bäuerle, D. *Appl. Phys. Lett.* **2002**, *80*, 4693. (b) Huang, S. M.; Sun, Z.; Lukyanchuk, B. S.; Hong, M. H.; Shi, L. P. *Appl. Phys. Lett.* **2005**, *86*, 161911. (c) Piparia, R.; Rothe, E. W.; Baird, R. J. *Appl. Phys. Lett.* **2006**, *89*, 223113. (d) Huang, S. M.; Sun, Z.; Lu, Y. F. *Nanotechnology* **2007**, *18*, 025302. (e) Lu, Y.; Chen, S. C. *Nanotechnology* **2003**, *14*, 505. (f) Yi, D. K.; Kim, M. J.; Turner, L.; Breuer, K. S.; Kim, D. Y. *Biotechnol. Lett.* **2006**, *28*, 169. (g) Chen, X.; Chen, Z. M.; Fu, N.; Lu, G.; Yang, B. *Adv. Mater.* **2003**, *15*, 1413. (h) Yan, Q.; Liu, F.; Wang, L.; Lee, J. Y.; Zhao, X. S. *J. Mater. Chem.* **2006**, *16*, 2132. (i) Choi, D.-G.; Jang, S. G.; Kim, S.; Lee, E.; Han, C.-S.; Yang, S.-M. *Adv. Funct. Mater.* **2006**, *16*, 33. (j) Choi, D.-G.; Yu, H. K.; Jang, S. G.; Yang, S.-M. *J. Am. Chem. Soc.* **2004**, *126*, 7019. (k) Zhang, G.; Wang, D. Y.; Möhwald, H. *Angew. Chem., Int. Ed.* **2005**, *44*, 7767. (l) Zhang, G.; Wang, D. Y.; Möhwald, H. *Nano Lett.* **2007**, *7*, 127.

(24) (a) Wang, X.; Lao, C.; Graugnard, E.; Summers, C. J.; Wang, Z. L. *Nano Lett.* **2005**, *5*, 1784. (b) Yan, F.; Goedel, W. A. *Nano Lett.* **2004**, *4*, 1193. (c) Duan, G. T.; Cai, W. P.; Luo, Y. Y.; Li, Z. G.; Lei, Y. *J. Phys. Chem. B* **2006**, *110*, 15729. (d) Duan, G. T.; Cai, W. P.; Luo, Y. Y.; Li, Y.; Lei, Y. *Appl. Phys. Lett.* **2006**, *89*, 181918. (e) Li, Y.; Cai, W. P.; Duan, G. T.; Cao, B. Q.; Sun, F. Q. *J. Mater. Res.* **2005**, *20*, 338. (f) Venkatesh, S.; Jiang, P. *Langmuir* **2007**, *23*, 8231.

(25) (a) Huang, Z. P.; Carnahan, D. L.; Rybczynski, J.; Giersig, M.; Sennett, M.; Wang, D. Z.; Wen, J. G.; Kempa, K.; Ren, Z. F. *Appl. Phys. Lett.* **2003**, *82*, 460. (b) Wang, Y.; Rybczynski, J.; Wang, D. Z.; Kempa, K.; Ren, Z. F.; Li, W. Z.; Kimball, B. *Appl. Phys. Lett.* **2004**, *85*, 4741. (c) Kempa, K.; Kimball, B.; Rybczynski, J.; Huang, Z. P.; Wu, P. F.; Steeves, D.; Sennett, M.; Giersig, M.; Rao, D. V. G. L. N.; Carnahan, D. L.; Wang, D. Z.; Lao, J. Y.; Li, W. Z.; Ren, Z. F. *Nano Lett.* **2003**, *3*, 13. (d) Park, K. H.; Lee, S.; Koh, K. H. J. *Appl. Phys.* **2005**, *97*, 024311.

(26) (a) Wang, X.; Summers, C. J.; Wang, Z. L. *Nano Lett.* **2004**, *4*, 423. (b) Liu, D. F.; Xiang, Y. J.; Wu, X. C.; Zhang, Z. X.; Liu, L. F.; Song, L.; Zhao, X. W.; Luo, S. D. W.; Ma, J.; Shen, J.; Zhou, W. Y.; Wang, G.; Wang, C. Y.; Xie, S. S. *Nano Lett.* **2006**, *6*, 2357. (c) Huang, Z.; Fang, H.; Zhang, J. *Adv. Mater.* **2007**, *19*, 744. (d) Fan, H. J.; Fuhrmann, B.; Scholz, R.; Syrowatka, F.; Dadgar, A.; Krost, A.; Zacharias, M. *J. Cryst. Growth* **2006**, *287*, 34. (e) Peng, K.; Zhang, M.; Lu, A.; Wong, N. B.; Zhang, R.; Lee, S. T. *Appl. Phys. Lett.* **2007**, *90*, 163123. (f) Wang, X. D.; Neff, C.; Graugnard, E.; Ding, Y.; King, J. S.; Pranger, L. A.; Tannenbaum, R.; Wang, Z. L.; Summers, C. J. *Adv. Mater.* **2005**, *17*, 2103. (g) Wang, X. D.; Song, J. H.; Wang, Z. L. *J. Mater. Chem.* **2007**, *17*, 711.

(27) (a) Kuo, C.-W.; Shiu, J.-Y.; Chen, P. *Chem. Mater.* **2003**, *15*, 2917. (b) Kuo, C.-W.; Shiu, J.-Y.; Cho, Y.-H.; Chen, P. *Adv. Mater.* **2003**, *15*, 1065. (c) Ladenburger, A.; Reiser, A.; Konle, J.; Feneberg, M.; Sauer, R.; Thonke, K.; Yan, F.; Goedel, W. A. *J. Appl. Phys.* **2007**, *101*, 03402. (d) Zhou, C. M.; Gall, D. *Appl. Phys. Lett.* **2007**, *90*, 093103. (e) Cheung, C. L.; Nikolic, R. J.; Reinhardt, C. E.; Wang, T. F. *Nanotechnology* **2006**, *17*, 1339. (f) Sinitskii, A.; Neumeier, S.; Nelles, J.; Fischler, M.; Simon, U. *Nanotechnology* **2007**, *18*, 305307. (g) Jiang, P. *Langmuir* **2006**, *22*, 3955.

(28) Jang, S. G.; Yu, H. K.; Choi, D.-G.; Yang, S. M. *Chem. Mater.* **2006**, *18*, 6103.

(29) (a) Kesapragada, S. V.; Gall, D. *Thin Solid Films* **2006**, *494*, 234. (b) Zhou, C. M.; Gall, D. *Appl. Phys. Lett.* **2006**, *88*, 203117. (c) Kosiorek, A.; Kandulski, W.; Chudzinski, P.; Kempa, K.; Giersig, M. *Nano Lett.* **2004**, *4*, 1359. (d) Zhou, C. M.; Gall, D. *J. Vac. Sci. Technol., A* **2007**, *25*, 312. (e) Zhou, C. M.; Gall, D. *Appl. Phys. Lett.* **2007**, *90*, 093103.

(30) Li, Y.; Cai, W. P.; Cao, B. Q.; Duan, G. T.; Sun, F. Q. *Polymer* **2005**, *46*, 12033.

(31) (a) Li, Y.; Cai, W. P.; Cao, B. Q.; Duan, G. T.; Sun, F. Q.; Li, C. C.; Jia, L. C. *Nanotechnology* **2006**, *17*, 238. (b) Li, Y.; Cai, W. P.; Duan, G. T.; Cao, B. Q.; Sun, F. Q.; Lu, F. *J. Colloid Interface Sci.* **2005**, *287*, 634. (c) Li, Y.; Duan, G. T.; Cai, W. P. *J. Colloid Interface Sci.* **2007**, *314*, 615. (d) Li, Y.; Li, C. C.; Cho, S. O.; Duan, G. T.; Cai, W. P. *Langmuir* **2007**, *23*, 9802.

(32) Pacifico, J.; Endo, K.; Morgan, S.; Mulvaney, P. *Langmuir* **2006**, *22*, 11072.

(33) Sun, F. Q.; Yu, J. C. *Angew. Chem., Int. Ed.* **2007**, *46*, 773.

(34) Xiu, Y. H.; Zhu, L. B.; Hess, D. W.; Wong, C. P. *Langmuir* **2006**, *22*, 9676.

(35) (a) Li, Y.; Huang, X. J.; Heo, S. H.; Li, C. C.; Choi, Y. K.; Cai, W. P.; Cho, S. O. *Langmuir* **2007**, *23*, 2169. (b) Huang, X. J.; Li, Y.; Im, H. S.; Yarimaga, O.; Kim, H. J.; Jang, D. Y.; Cho, S. O.; Cai, W. P.; Choi, K. Y. *Nanotechnology* **2006**, *17*, 2988. (c) Correa-Duarte, M. A.; Kosiorek, A.; Kandulski, W.; Giersig, M. *Small* **2006**, *2*, 220.

(36) Li, Y.; Lee, E. J.; Cho, S. O. *J. Phys. Chem. C* **2007**, *111*, 14813.

(37) (a) Haes, A. J.; Van Duyne, R. P. *J. Am. Chem. Soc.* **2002**, *124*, 10596. (b) Riboh, J. C.; Haes, A. J.; McFarland, A. D.; Yonzon, C. R.; Van Duyne, R. P. *J. Phys. Chem. B* **2003**, *107*, 1772. (c) Zhang, X.; Hicks, E. M.; Zhao, J.; Schatz, G. C.; Van Duyne, R. P. *Nano Lett.* **2005**, *5*, 1503. (d) Yonzon, C. R.; Jeoung, E.; Zou, S.; Schatz, G. C.; Mrksich, M.; Van Duyne, R. P. *J. Am. Chem. Soc.* **2004**, *126*, 12669.

(38) (a) Haynes, C. L.; Van Duyne, R. P. *J. Phys. Chem. B* **2003**, *107*, 7426. (b) Zhang, X.; Yonzon, C. R.; Van Duyne, R. P. *J. Mater. Res.* **2006**, *21*, 1083. (c) Lu, L.; Randjelovic, I.; Capek, R.; Gaponik, N.; Yang, J.; Zhang, H.; Eychmuller, A. *Chem. Mater.* **2005**, *17*, 5731.

CM701977G